Rapid early Holocene deglaciation of the Laurentide ice sheet

ANDERS E. CARLSON[1]*, ALLEGRA N. LEGRANDE[2], DELIA W. OPPO[3], ROSEMARIE E. CAME[4], GAVIN A. SCHMIDT[2], FARON S. ANSLOW[5], JOSEPH M. LICCIARDI[6] AND ELIZABETH A. OBBINK[1]

[1]Department of Geology and Geophysics, University of Wisconsin, Madison, Wisconsin 53706, USA
[2]NASA Goddard Institute for Space Studies and Center for Climate System Research, Columbia University, New York 10025, USA
[3]Department of Geology and Geophysics, Woods Hole Oceanographic Institution, Woods Hole, Massachusetts 02543, USA
[4]Geology and Planetary Sciences, California Institute of Technology, Pasadena, California 91125, USA
[5]Earth and Ocean Sciences, University of British Columbia, Vancouver, BC, V6T 1Z4, Canada
[6]Department of Earth Sciences, University of New Hampshire, Durham, New Hampshire 03824, USA
*e-mail: acarlson@geology.wisc.edu

Published online: 31 August 2008; doi:10.1038/ngeo285

The demise of the Laurentide ice sheet during the early Holocene epoch is the most recent and best constrained disappearance of a large ice sheet in the Northern Hemisphere, and thus allows an assessment of rates of ice-sheet decay as well as attendant contributions to sea level rise. Here, we use terrestrial and marine records of the deglaciation to identify two periods of rapid melting during the final demise of the Laurentide ice sheet, when melting ice contributed about 1.3 and 0.7 cm of sea level rise per year, respectively. Our simulations with a fully coupled ocean–atmosphere model suggest that increased ablation due to enhanced early Holocene boreal summer insolation was the predominant cause of Laurentide ice-sheet retreat. Although the surface radiative forcing in boreal summer during the early Holocene is twice as large as the greenhouse-gas forcing expected by the year 2100, the associated increase in summer surface air temperatures is very similar. We conclude that our geologic evidence for a rapid retreat of the Laurentide ice sheet may therefore describe a prehistoric precedent for mass balance changes of the Greenland ice sheet over the coming century.

One of the greatest sources of uncertainty in projections of future sea level rise in response to global warming is the contribution from the Greenland ice sheet[1] (GIS). This uncertainty arises in part because the period of direct observations available to create empirical predictions and to test the current generation of ice-sheet models is extremely short[1–5]. Examination of past ice-sheet–climate interactions provides a record of ice-sheet growth and decay longer than modern observations. In particular, the behaviour of terrestrial ice sheets under climates warmer than present affords potential insight into the future behaviour of the GIS. During the early Holocene epoch, enhanced boreal summer insolation[6] (Fig. 1a) warmed Northern Hemisphere summers by several degrees, presumably driving retreat of the Laurentide ice sheet[7–9] (LIS). However, portions of the northern and eastern North Atlantic were colder than present[10–12], possibly as a consequence of the suppression of Labrador Sea deep-water production by LIS melt water[13,14]. The gradual rise in sea level during the early Holocene[15–17] was punctuated by at least two increases in the rate of sea level rise, which were sourced from either the LIS or the Antarctic ice sheet, indicating variations in the rate of ice-sheet melting[14,18,19]. The early Holocene LIS thus represents the most recent disappearance of a mid- to high-latitude terrestrial ice sheet, and can provide constraints on how fast terrestrial ice sheets can melt and raise sea level under a climate warmer than present.

EARLY HOLOCENE LIS RETREAT

To determine the LIS retreat rate, we compiled minimum-limiting radiocarbon dates of deglaciation for Quebec, Labrador, eastern Nunavut[20] and Hudson Bay[21], along with cosmogenic ^{10}Be ages from Labrador[22] and Quebec[14] (Figs 1c, 2a and Supplementary Information, Fig. S1). All radiocarbon ages are calibrated, reservoir corrected if marine[20,21] (Supplementary Information, Table S1), and presented as straight averages of the oldest dates, which constrain deglaciation as occurring sometime before the deposition of the organic material or shell.

Four marine shell dates place the marine incursion following deglaciation of the northern bank of the St. Lawrence estuary at 11.8 ± 0.3 kyr BP (see Supplementary Information, Fig. S1). The southern LIS margin may have stabilized near the St. Lawrence estuary, because the oldest terrestrial organic material from southeastern Quebec dates to 8.7 ± 0.3 kyr BP (two dates). Farther east, the southern Labrador coast deglaciated before 11.2 ± 0.4 kyr BP (two marine dates) with the ice margin possibly remaining near the coast until sometime before 8.6 ± 0.7 kyr BP (two terrestrial dates). Along the northeastern side of the LIS, ^{10}Be dates indicate ice retreat from the northeastern Labrador coastal moraines at 13.4 ± 1.5 kyr BP (seven dates) and 12.0 ± 2.1 kyr BP (six dates)[22]. The oldest terrestrial radiocarbon dates from near the coast indicate that ice may have persisted there until

© 2008 Macmillan Publishers Limited. All rights reserved.

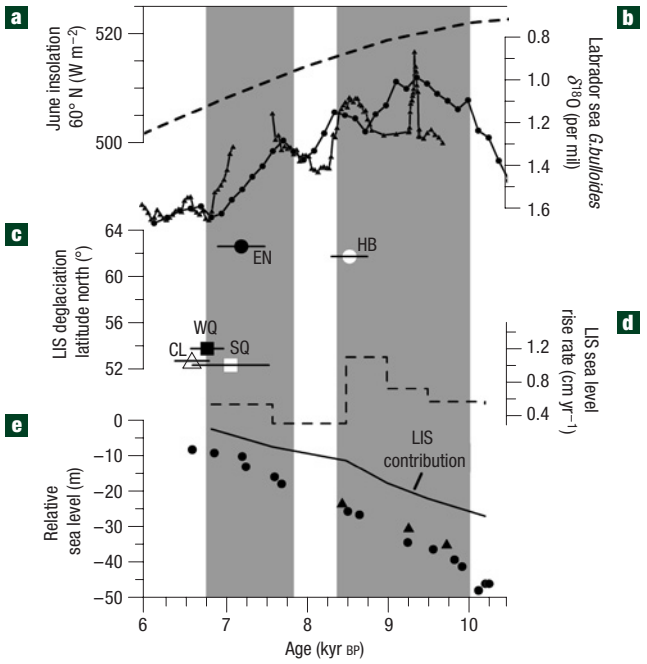

Figure 1 Early Holocene terrestrial and marine records. a, 60° N June insolation[6]. **b**, *G. bulloides* $\delta^{18}O_{calcite}$ records with ice volume removed[16] from southwestern Labrador Sea (circles: MD95-2024, 50.21° N, 45.69° W, water depth 3,539 m (ref. 24), triangles: MD99-2237, 50.20° N, 45.68° W, water depth 3,530 m (ref. 25)). **c**, LIS deglaciation relative to latitude north. HB: Hudson Bay[21], WQ: western Quebec[14], SQ: southern Quebec[20], CL: central Labrador[20], EN: eastern Nunavut[20]. **d**, Rate of sea level rise from the LIS. **e**, Relative sea level data (triangles from Barbados[16], circles from Tahiti[17]) and changes in LIS volume (black line). Grey bars denote periods of increased LIS melting.

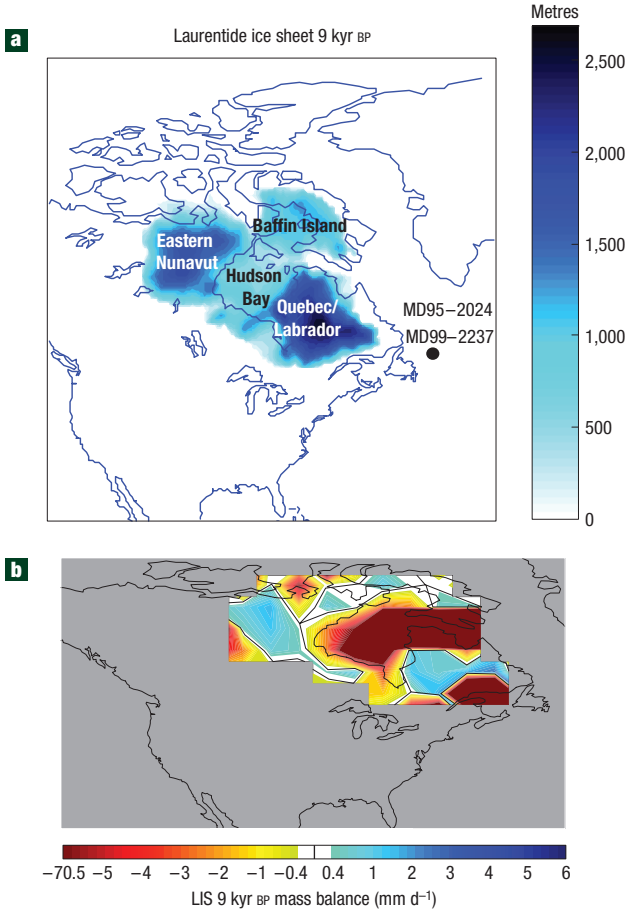

Figure 2 LIS topography and mass balance. a, LIS topography[7] (m) used as AOGCM input with regions labelled and the locations of MD95-2024 & MD99-2237. **b**, ModelE-R-simulated annual mass balance predicted (mm d^{-1}) with the black lines denoting the equilibrium line.

9.9 ± 0.3 kyr BP (six dates). In contrast, ice over Hudson Bay and the western LIS margin continued to thin and retreat during the early Holocene with the only firm chronologic constraint being the collapse of ice over Hudson Bay 8.5 ± 0.2 kyr BP (ref. 21).

Following this collapse, the LIS split into two ice caps: one over Quebec and Labrador, the second over eastern Nunavut and Baffin Island (Fig. 2a). A gap in minimum-limiting radiocarbon ages suggests the Quebec/Labrador ice cap margins subsequently stabilized. The southern Quebec margin resumed northward retreat before 7.5 ± 0.2 kyr BP (three dates) and southern to central Quebec deglaciated before 7.1 ± 0.1 kyr BP (two dates). Three dates from eastern Labrador indicate ice-margin retreat resumed before 7.5 ± 0.1 kyr BP, and western to central Labrador deglaciated before 6.6 ± 0.4 kyr BP (three dates). Thirteen ^{10}Be dates and the timing of the marine limit from western Quebec suggest a similar retreat history, with deglaciation of the James Bay coast by 8.0 ± 0.2 kyr BP followed by margin stabilization[14]. The western margin resumed retreat ~7.4 kyr BP with deglaciation across western to central Quebec 6.8 ± 0.2 kyr BP (ref. 14). To the northwest, three marine shell dates place the marine incursion in northeastern Nunavut at 7.2 ± 0.1 kyr BP, indicating deglaciation before the incursion. Small ice caps probably persisted over northern Quebec and Labrador until sometime before 5.7 ± 0.2 kyr BP (four dates) and 5.5 ± 0.2 kyr BP (one date), respectively, and ice over Baffin Island continued to retreat until ~6 kyr BP (ref. 23). These small ice caps probably constituted <0.5 m of sea level rise[7].

On the basis of the above chronology, we suggest that two intervals of retreat and enhanced melting of the LIS occurred in the early Holocene, and place the end of significant LIS melting at 6.8 ± 0.3 kyr BP (Fig. 1c). The onset of the first enhanced retreat period presumably began after the Younger Dryas cold event ended ~11.5 kyr BP and more likely closer to ~9 kyr BP on the basis of the radiocarbon dates, culminating in the opening of Hudson Bay ~8.5 kyr BP (Supplementary Information, Fig. S2). Much of this early melting was probably focused along the southwestern to western LIS margin and over Hudson Bay, possibly related to the 0.4–0.6‰ decrease in Labrador Sea planktonic $\delta^{18}O$ (*Globigerina bulloides*) (reduced surface water density)[24–26] at ~10–8.4 kyr BP with peak $\delta^{18}O$ depletion ~9 kyr BP (Fig. 1b). After a period of margin stabilization, which may represent a response to regional reorganization of atmospheric circulation patterns following the opening of Hudson Bay[14] and cooling from the drainage of glacial Lake Agassiz with attendant reduced Atlantic meridional overturning circulation[12,21,25–27] (AMOC), retreat of the LIS resumed ~7.6 kyr BP and ended ~6.8 kyr BP (Supplementary Information, Fig. S2). This latter period of melting may also be reflected in the Labrador Sea as a 0.2–0.3‰ decrease in $\delta^{18}O$ (Fig. 1b).

LIS CONTRIBUTIONS TO SEA LEVEL RISE

We estimate the LIS Holocene sea level rise contribution by converting LIS area[20] (km^2), with revised area ages matching our

© 2008 Macmillan Publishers Limited. All rights reserved.

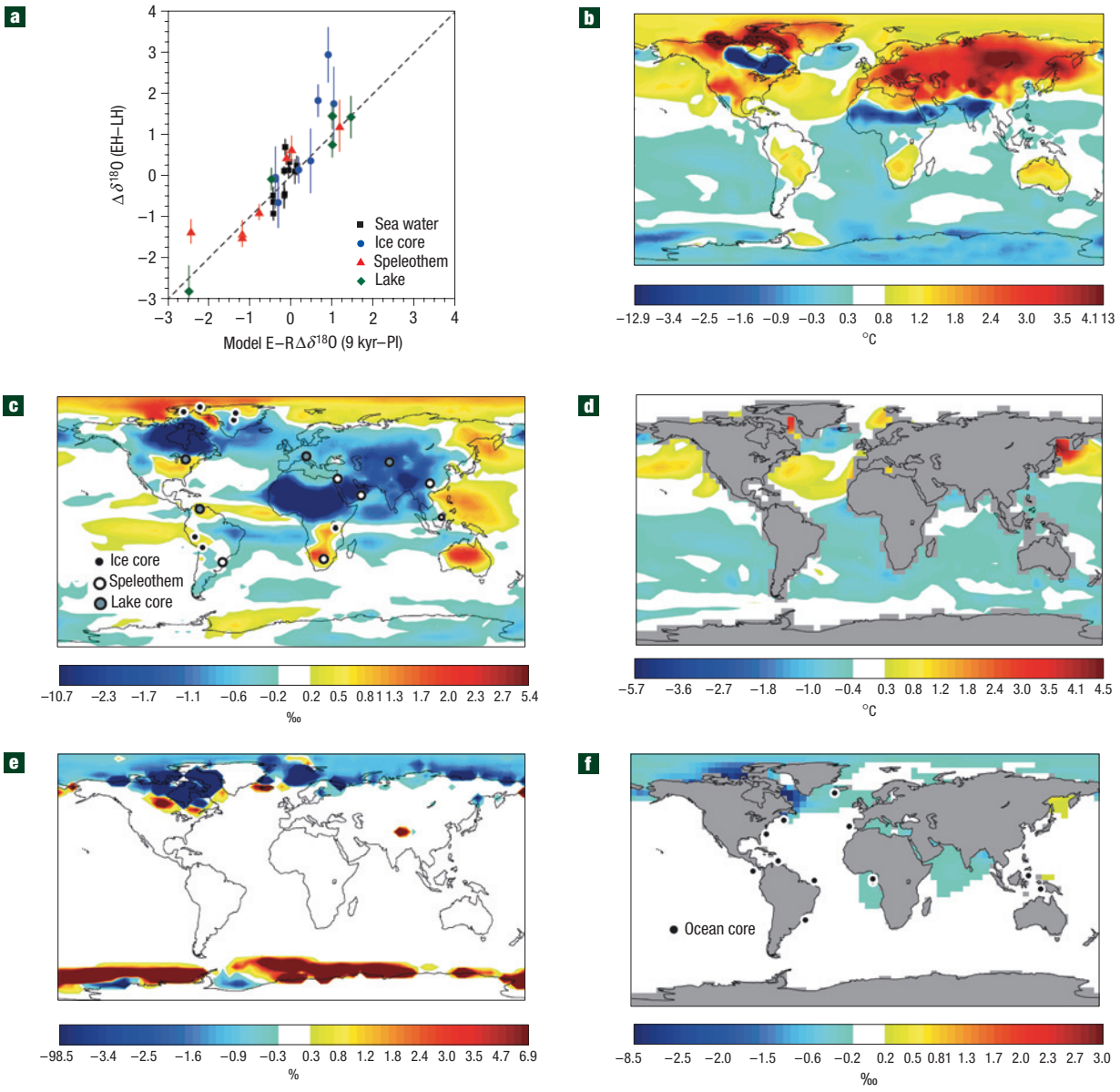

Figure 3 ModelE-R Output Delta Maps between 9 kyr BP and the pre-industrial era. a, Comparison between palaeo-$\Delta\delta^{18}O$ precipitation and seawater changes between the early Holocene (EH) and late Holocene (LH) (see **c** and **e** for locations) and ModelE-R 9-kyr-BP–pre-industrial (PI) predicted changes. Dashed line is 1:1 relationship. See Supplementary Information, Table S2 for data. **b**, ModelE-R ΔSAT summer. **c**, ModelE-R $\Delta\delta^{18}O_{precipitation}$ annual (ice volume removed). **d**, ModelE-R Δ sea surface temperature. **e**, ModelE-R Δ summer sea-ice extent. **f**, ModelE-R $\Delta\delta^{18}O_{sw}$ annual (ice volume removed).

LIS chronology (see Supplementary Information, Fig. S2), to ice volume (km^3) using the well-established relationship for an ice sheet on a hard bed[28] ($\log[\text{volume}] = 1.23[\log[\text{area}] - 1]$). Although this assumes an ice sheet is in equilibrium, this relationship was developed on ice sheets and ice caps with both negative and positive mass balances, single and multiple ice domes, a span four orders of magnitude in area (Antarctic ice sheet to the Barnes ice cap) and climate conditions from temperate maritime (Iceland) to polar desert (Antarctica). The error in the volume estimate is ~12%, which places the empirically predicted 11 kyr BP ice volume in agreement with LIS volumes reconstructed by a physically based steady-state ice-sheet model[7] and an isostatic rebound model[15].

From 11 to 6 kyr BP, sea level rose at an average rate of ~1 cm yr^{-1}, largely reflecting melting of the LIS and the Antarctic ice sheet, with higher rates during the early Holocene than mid-Holocene[15–17] (Fig. 1e). Between 11 and 9 kyr BP, we estimate the LIS contributed 15 ± 1.8 m of sea level rise at 0.7–0.9 cm yr^{-1} (Fig. 1d,e). During the subsequent phase of rapid LIS retreat 9–8.5 kyr BP, the LIS contributed 6.6 ± 0.8 m of sea level rise at ~1.3 cm yr^{-1}. This rate is comparable to geologic evidence for global sea level rise for this interval derived from coral records[16,17] (Fig. 1d). Estuarine records from Chesapeake Bay[18] also indicate a marsh drowning event ~8.9 kyr BP not explained by isostasy with sea level rising at $\geqslant$1.2 cm yr^{-1}, similar to our estimated rate of sea level rise from the LIS. After 8.5 kyr BP, the remaining 9.2 ± 1.1 m of LIS sea level rise was added over ~1.7 kyr. The LIS chronology and Labrador Sea $\delta^{18}O$ records suggest a deceleration of retreat ~8.5–7.6 kyr BP with a subsequent increase, corresponding to a

© 2008 Macmillan Publishers Limited. All rights reserved.

LIS contribution to sea level rise of ~0.4 cm yr^{-1} 8.5–7.6 kyr BP, increasing to ~0.7 cm yr^{-1} 7.6–6.8 kyr BP (Fig. 1d). Accelerated LIS retreat 7.6–6.8 kyr BP corresponds with a second increase in the rate of Holocene sea level rise ~7.6 kyr BP (ref. 19), when sea level rose ~4.5 m at ~1.0 cm yr^{-1}, suggesting that the LIS was also the main source of sea level rise at this time[14].

IMPACT OF EARLY HOLOCENE CLIMATE ON THE LIS

To quantify the effects of enhanced boreal summer insolation on the LIS and climate, we simulated the 9 kyr BP climate, with a prescribed LIS (ref. 7) (Fig. 2a), using the fully coupled atmosphere–ocean general circulation model (AOGCM), NASA Goddard Institute for Space Studies ModelE-R[29]. This model contains a fully coupled surface energy and moisture balance over land ice, but does not include any horizontal ice advection, limiting our analysis to the estimation of the LIS surface mass balance. In addition, the model tracks water isotopes throughout the hydrologic cycle[29]. To test the skill of the model at simulating 9 kyr BP climate, we compared simulated $\Delta\delta^{18}$O (9 kyr BP—pre-industrial[29]) against a compilation of $\Delta\delta^{18}$O from geologic data (Fig. 3c,f). We compiled early Holocene (8–10 kyr BP) and late Holocene (3–0 kyr BP) δ^{18}O from ice cores, lake cores and speleothems, and estimated seawater δ^{18}O ($\delta^{18}O_{sw}$) from paired Mg/Ca-based sea surface temperature and $\delta^{18}O_{calcite}$ measurements on the calcite shells of planktonic foraminifera (Supplementary Information for a full discussion of methods of data model comparison and model results). Simulated $\Delta\delta^{18}$O are in agreement with the early Holocene–late Holocene $\Delta\delta^{18}$O ($R^2 = 0.83$) (Fig. 3a). Given the coarse resolution of the AOGCM, this correlation between data and predictions provides confidence in the ability of the model to simulate regional aspects of 9 kyr BP climate, hydrology and LIS surface mass balance.

ModelE-R simulates low $\delta^{18}O_{sw}$ (Fig. 3f), $\delta^{18}O_{calcite}$ and reduced sea surface salinity (not shown) across the northern North Atlantic, Labrador Sea and Arctic Ocean related to the negative LIS mass balance and enhanced runoff, in agreement with North Atlantic palaeohydrology data[12–14,26]. The alteration in ocean density suppresses deep winter convection in the Labrador Sea, decreasing total AMOC by ~15% relative to present, also in agreement with interpretations of Labrador Sea deep-water proxies[13]. Reduced AMOC yields relatively cooler temperatures over the Labrador Sea (1–2 °C in the winter, 0.5–1 °C in the summer) extending eastward into the northern North Atlantic (Fig. 3b,d), matching early Holocene palaeoclimate reconstructions[10,11]. Further contributing to cooler temperatures is the influence of LIS elevation and albedo, with surface air temperature (SAT) up to 13.5 °C cooler over the ice sheet in the summer, of which 1–2 °C is due to the ice albedo effect (Fig. 3b). The high-pressure system over the LIS maintains an anti-cyclone, reversing wind patterns over Canada (Supplementary Information, Fig. S3a). The LIS topography forces the mid-latitude jet southward and increases the jet strength (Supplementary Information, Fig. S3b). Outside the northern North Atlantic, the Northern Hemisphere summer SST and SAT rise in response to enhanced boreal summer insolation (Fig. 3b,d), amplified by a ~5% reduction in Arctic summer sea ice (Fig. 3e).

The 9 kyr BP simulated annual LIS surface mass balance is −260 cm yr^{-1}, with accumulation zones centred over Quebec, Labrador and eastern Nunavut (Fig. 2b). Much of the LIS mass reduction is over Hudson Bay where low-elevation ice is lost at rates ranging 11–71 mm day^{-1}, in reasonable accord with our inferences from the LIS chronology. Integrating this LIS mass loss from 9 to 8.5 kyr BP results in ~6 m of sea level rise at ~1.3 cm yr^{-1}, similar to estimates from the LIS chronology (Fig. 1).

IMPLICATIONS FOR FUTURE SEA LEVEL RISE

The agreement between our interpretations from geologic data and the 9 kyr BP AOGCM that does not include ice dynamics suggests that ice sheets (the LIS) may have melted rapidly in the past. The inclusion of ice dynamics (for example, ice streaming) in the 9 kyr BP AOGCM would probably only enhance the melt rate[2]. However, by the early Holocene, much of the LIS was on a hard bed, where ice streaming is rare (but not absent), implying that ablation controlled LIS mass balance during this time interval. The AOGCM predicts that a boreal summer short-wave radiative forcing of ~40 W m^{-2} relative to present at the top of the atmosphere[6] can cause considerable summer warming (1–3 °C), promoting a negative mass balance and accelerated melting of a terrestrial ice sheet. Direct comparison to simulations of AD 2,100 climate (Special Report on Emissions scenario A1B)[1] is difficult because of a complicated suite of forcings including greenhouse gases, black carbon, ozone, snow albedo, atmospheric H_2O, aerosols and land use[30]. However, the cumulative effect is that the increased downward long-wave radiation over the GIS (~10 W m^{-2}) (ref. 30) is roughly half the surface short-wave radiation changes on the LIS at 9 kyr BP (~20 W m^{-2}), but the summer SAT warming (2–4 °C) (ref. 30) is similar in both cases.

In addition, the different sizes of the early Holocene LIS and the GIS combined with their geographical settings, though they both rest on hard beds predominately above sea level, complicate direct inferences. The GIS is situated in the centre of the North Atlantic with a greater portion of its margin terminating near the ocean, whereas only the eastern and northern LIS margins were near the coast, with the southwestern margin terminating in proglacial lakes. The modern GIS is also ~3 times smaller than the LIS at the start of the Holocene[7,15], but the LIS was similar in size ~8 kyr BP. At present, ablation, ice streaming and calving control GIS mass loss[2]. However, ice streaming and calving will decrease or cease if the GIS retreats inland[4], making it more analogous to the LIS (ref. 7). Nevertheless, predictions of the rate of sea level rise from the GIS by the end of this century in the A1B scenario[1] are 6–40 times smaller than the estimated rate of LIS mass loss in the early Holocene. Given the similar summer SAT responses for these two periods, and the geologic evidence for rapid early Holocene LIS retreat, current projections of GIS melt rates for the coming century may be only minimum estimates even without considering positive feedbacks from ice-sheet dynamics.

METHODS

We simulate climate using the fully coupled AOGCM NASA Goddard Institute for Space Studies ModelE-R, which includes water isotopes[29], permitting direct comparison to marine and terrestrial δ^{18}O records. Because a true transient simulation from the Last Glacial Maximum—even assuming that the glacial maximum was in equilibrium—to 9 kyr BP is beyond our current computational power, we carried out a time-slice simulation of 9 kyr BP climate. Boundary conditions appropriate to 9 kyr BP are prescribed (greenhouse gases, insolation, LIS topography, 40 m of sea level lowering and its effects on ocean salinity and δ^{18}O, and the addition of glacial Lake Agassiz), with details provided in the Supplementary Information. ModelE-R has a simple ice-sheet scheme that includes ice-sheet surface albedo and energy, fresh water and water isotopes, with two snow/ice layers that transfer heat and mass. Net melt is transported through a 9-kyr-BP-appropriate river routing scheme based on LIS topography and North American isostasy[7]. Ideally, a higher-resolution model with ice dynamics would be used, but these usually use simplified predictions of summer melt and are asynchronously coupled to GCMs (refs 3,4), not allowing the ice-sheet hydrology to directly communicate with the atmosphere and ocean systems. Within the model, there is an imposed global water balance, which modulates the ice calving term to prevent long-term salinity drift in the ocean, with the Southern and Northern hemispheres partitioned separately. Thus, in the model experiment, the negative LIS surface mass balance is

© 2008 Macmillan Publishers Limited. All rights reserved.

compensated by a reduction in Northern Hemisphere iceberg calving from the GIS, and therefore, probably underestimates the total ice-sheet impact on ocean outflow. ModelE-R was run for 600 model years with results from the last 100 years averaged and compared to a corresponding 100-year average of the pre-industrial era[29]. Differences between 9 kyr BP and the pre-industrial era[29] were calculated using a student-*t* test at 99% confidence.

Received 3 April 2008; accepted 28 July 2008; published 31 August 2008.

References

1. Solomon, S. D., Manning, M. & Qin, D. (eds) *Climate Change 2007: The Physical Basis 4th Assessment Report, IPCC* 18 (Cambridge Univ. Press, Cambridge, 2007).
2. Alley, R. B., Clark, P. U., Huybrechts, P. & Joughin, I. Ice-sheet and sea-level changes. *Science* **310**, 456–460 (2005).
3. Wild, M., Calanca, P., Scherrer, S. C. & Ohmura, A. Effects of polar ice sheets on global sea level in high-resolution greenhouse scenarios. *J. Geophys. Res.* **108**, doi:10.1029/2002JD002451 (2003).
4. Ridley, J. K., Huybrechts, P., Gregory, J. M. & Lowe, J. A. Elimination of the Greenland Ice Sheet in a high CO_2 climate. *J. Clim.* **18**, 3409–3427 (2005).
5. Gregory, J. M., Huybrechts, P. & Raper, S. C. B. Threatened loss of the Greenland ice-sheet. *Nature* **428**, 616. (2004).
6. Berger, L. & Loutre, M. F. Insolation values for the climate of the last 10 million years. *Quat. Sci. Rev.* **17**, 211–219 (1991).
7. Licciardi, J. M., Clark, P. U., Jenson, J. W. & MacAyeal, D. R. Deglaciation of a soft-bedded Laurentide Ice Sheet. *Quat. Sci. Rev.* **17**, 427–488 (1998).
8. Mitchell, J. F. B., Grahame, N. S. & Needham, K. J. Climate simulations for 9000 years before present: Seasonal variations and effect of the Laurentide Ice Sheet. *J. Geophys. Res. Atmos.* **93**, 8283–8303 (1988).
9. Pollard, D., Bergengren, J. C., Stillwell-Soller, L. M., Felzer, B. & Thompson, S. L. Climate simulations for 10,000 and 6,000 years BP. *Paleoclimates* **2**, 183–218 (1998).
10. Kaufman, D. S. *et al*. Holocene thermal maximum in the western Arctic (0–180° W). *Quat. Sci. Rev.* **23**, 529–560 (2004).
11. Kaplan, M. R. & Wolfe, A. P. Spatial and temporal variability of Holocene temperature in the north Atlantic. *Quat. Res.* **65**, 223–231 (2006).
12. Came, R. E., Oppo, D. W. & McManus, J. F. Amplitude and timing of temperature and salinity variability in the subpolar North Atlantic over the past 10 k.y. *Geology* **35**, 315–318 (2007).
13. Hillaire-Marcel, C., de Vernal, A., Bilodeau, G. & Weaver, A. J. Absence of deep-water formation in the Labrador Sea during the last interglacial period. *Nature* **410**, 1073–1077 (2001).
14. Carlson, A. E., Clark, P. U., Raisbeck, G. M. & Brook, E. J. Rapid Holocene deglaciation of the Labrador sector of the Laurentide Ice Sheet. *J. Clim.* **20**, 5126–5133 (2007).
15. Peltier, W. R. Global glacial isostasy and the surface of the ice-age Earth: The ICE-5G (VM2) Model and GRACE. *Annu. Rev. Earth Planet. Sci* **32**, 111–149 (2004).
16. Fairbanks, R. G. A 17,000 year glacio-eustatic sea level record: Influence of glacial melting rates on the Younger Dryas event and deep ocean circulation. *Nature* **342**, 637–642 (1989).
17. Bard, E. B. *et al.* Deglacial sea-level record from Tahiti corals and the timing of global meltwater discharge. *Nature* **382**, 241–244 (1996).
18. Cronin, T. M. *et al*. Rapid sea level rise and ice sheet response to 8,200-year climate event. *Geophys. Res. Lett.* **34**, doi:10.1029/2007GL031318 (2007).
19. Yu, S.-Y., Berglund, B. E., Sandgren, P. & Lambeck, K. Evidence for a rapid sea-level rise 7600 yr ago. *Geology* **35**, 891–894 (2007).
20. Dyke, A. S. in *Quaternary Glaciations-Extent and Chronology Part II* Vol. 2b (eds Ehlers, J. & Gibbard, P. L.) 373–424 (Elsevier, Amsterdam, 2004).
21. Barber, D. C. *et al*. Forcing of the cold event of 8,200 years ago by catastrophic drainage of Laurentide lakes. *Nature* **400**, 344–348 (1999).
22. Clark, P. U., Brook, E. J., Raisbeck, G. M., Yiou, F. & Clark, J. Cosmogenic ^{10}Be ages of the Saglek Moraines, Torngat Mountains, Labrador. *Geology* **31**, 617–620 (2003).
23. Miller, G. H., Wolfe, A. P., Briner, J. P., Sauer, P. E. & Nesje, A. Holocene glaciation and climate evolution of Baffin Island, Arctic Canada. *Quat. Sci. Rev.* **24**, 1703–1721 (2005).
24. Hillaire-Marcel, C. & Bilodeau, G. Instabilities in the Labrador Sea water mass structure during the last climatic cycle. *Can. J. Earth Sci.* **37**, 795–809 (2000).
25. Hillaire-Marcel, C., de Vernal, A. & Piper, D. J. W. Lake Agassiz final drainage event in the northwest North Atlantic. *Geophys. Res. Lett.* **34**, doi:10.1029/2007GL030396 (2007).
26. Keigin, L. D., Sachs, J. P., Rosenthal, Y. & Boyle, E. A. The 8200 year B.P. event in the slope water system, western subpolar north Atlantic. *Paleoceanography* **20**, doi:10.1029/2004PA001074 (2005).
27. LeGrande, A. N. *et al*. Consistent simulations of multiple proxy responses to an abrupt climate change event. *Proc. Natl Acad. Sci.* **103**, 837–842 (2006).
28. Paterson, W. S. B. *The Physics of Glaciers* (Butterworth-Heinemann, Oxford, 1994).
29. Schmidt, G. A., LeGrande, A. N. & Hoffmann, G. Water isotope expressions of intrinsic and forced variability in a coupled ocean-atmosphere model. *J. Geophys. Res. Atmos.* **112**, doi:10.1029/2006JD007781 (2007).
30. Hansen, J. *et al*. Dangerous human-made interferences with climate: a GISS modelE study. *Atmos. Chem. Phys.* **7**, 2287–2312 (2007).

Supplementary Information accompanies this paper on www.nature.com/naturegeoscience.

Acknowledgements

We would like to thank J. Stoner for discussion of Orphan Knoll cores, and L. Keigwin and L. Skinner for sharing data. This research was financially supported by National Science Foundation grants ATM-05-01351 & ATM-05-01241 to D.W.O. and G.A.S., start-up funds from the University of Wisconsin-Madison and a Woods Hole Oceanographic Institution Postdoctoral Scholarship to A.E.C., and the Woods Hole Oceanographic Institution's Ocean and Climate Change Institute (D.W.O. and R.E.C.).

Author contributions

A.E.C. compiled terrestrial and marine records of LIS retreat. A.N.L. and G.A.S. developed the AOGCM model. A.N.L. initiated and analysed the 9 kyr BP simulations. A.N.L., G.A.S., A.E.C. and J.M.L. designed model boundary conditions. A.E.C., R.E.C., E.A.O. and D.W.O. compiled oxygen isotope data. A.N.L., A.E.C. and F.S.A. interpreted LIS mass balance. All authors collaborated on the text.

Author information

Reprints and permission information is available online at http://npg.nature.com/reprintsandpermissions. Correspondence and requests for materials should be addressed to A.E.C.

© 2008 Macmillan Publishers Limited. All rights reserved.